

# Non-Parametric Machine Text Detection via Multi-View Gaussian Processes

Aleem Khan, Nicholas Andrews

Department of Computer Science

Johns Hopkins University

{aleem, noa}@cs.jhu.edu

## Abstract

Adversarial conditions such as paraphrasing and targeted style transfer sharply degrade the accuracy of machine text detectors. A document, however, carries multiple complementary signals (e.g., stylistic features, likelihood and rank-order features, and structural features), and an attack that suppresses one may leave others intact. While a parametric classifier can learn to combine these features given sufficient supervision, classifiers are prone to making confidently incorrect predictions when the distribution shifts (e.g., novel attacks or unseen language models). To address this, we propose a multi-view, non-parametric detection framework that extracts complementary feature views from the same document and aggregates per-view evidence through a Gaussian process ensemble. By aggregating evidence across views, an adversary must simultaneously defeat multiple independent axes of detection, substantially raising the cost of evasion. The Gaussian process formulation additionally provides calibrated probabilities and principled abstention on out-of-distribution inputs, supporting reliable deployment in high-stakes settings. We evaluate on three benchmarks spanning diverse generators and attacks: the DetectRL and RAID benchmarks, and the PAN 2025 shared task and demonstrate that our multi-view detector maintains strong performance under the considered attacks, outperforming existing approaches against held out attacks.

## 1 Introduction

As language models (LMs) have become more capable and widely available to users, text generated by LMs has become more ubiquitous and indistinguishable from human writing (Comanici et al., 2025; Grattafiori et al., 2024; OpenAI et al., 2024). While LMs serve many positive use cases, and have become closely intertwined with workflows, detection of machine-generated content, especially in high-stakes domains, is increasingly of interest to

many communities (Ippolito et al., 2020; Gehring and Paaßen, 2025). As generators have improved, detectors have as well: a growing body of work on machine-generated text detection, yielding zero-shot statistical tests (Bao et al., 2024; Gehrmann et al., 2019; Hans et al., 2024), trained classifiers (Li et al., 2024; Lee et al., 2024; Tian et al., 2024; Hu et al., 2023), and commercial detection services (Emi and Spero, 2024). Under controlled conditions, where machine text is generated without modification or adversarial intent, these detectors achieve high accuracy (Hans et al., 2024). However, real-world deployment introduces a fundamentally harder problem: adversarial conditions in which machine text is *edited, rewritten, or obfuscated*, with a human or another LM, before it reaches the detector (Thai et al., 2026).

Adversarial manipulation comes in many forms. In relatively simpler cases, a user may attempt to alter machine written documents with a prompt (Patel et al., 2024). On the other end of the spectrum, a more sophisticated adversary may fine-tune generators to target specific types of detector directly (Nicks et al., 2024), or through proxies (Wang et al., 2025; Soto et al., 2025). Alternatively, machine text may be passed through a trained paraphraser to disrupt rank order scores of tokens (Krishna et al., 2023), or a pipeline of multiple paraphrasers, which can amplify this degradation. These attacks exploit different vulnerabilities, but most existing detectors rely on a single feature space, such as token-level probability under a reference language model (Gehrmann et al., 2019), or stylistic fingerprints (Soto et al., 2024), and a targeted edit along that axis is sufficient to evade detection. To address the multi-objective nature of detection, we propose a multi-view, non-parametric framework that exploits this insight.

We begin by building a few-shot support for a target domain. Our method relies on having a small number of human and machine exemplars

from a domain of interest<sup>1</sup>. For each of  $K$  views (§3.1), we fit independent Gaussian process classifiers, yielding probabilities that naturally incorporate the GP’s predictive uncertainty (§3.3). These probabilities are aggregated via a secondary linear model which produces a final calibrated uncertainty (§3.4).

Our contributions are as follows: (1) A multi-view detection framework that aggregates complementary views for robust detection under human editing and paraphrase attacks. (2) A Gaussian process ensemble that delivers calibrated uncertainty, and thorough analysis demonstrating the approach’s robustness to various attacks. (3) Evaluation on diverse benchmarks: DetectRL and RAID benchmarks, and PAN 2025 shared task datasets, demonstrating strong performance under adversarial conditions where single-view detectors fail.

## 2 Preliminaries

### 2.1 Detection Under Adversarial Conditions Remains Difficult

Detection of AI-generated and AI-manipulated content has received significant attention from the research community as generators have become more capable and accessible. Zero-shot detection methods score documents using a reference model, using the idea that machine-generated text will generally be more likely under any language model (Mitchell et al., 2023; Bao et al., 2024; Hans et al., 2024; Su et al., 2023; Yang et al., 2024). Parametric methods have also demonstrated strong performance, but struggle to adapt to new distributions (Solaiman et al., 2019; Li et al., 2024; Hu et al., 2023). Watermarking has emerged as another effective approach for detection, but it assumes access to the model during inference (Kirchenbauer et al., 2023).

Recent work has also demonstrated that many detection approaches have significant vulnerabilities to a range of attacks and adversarial conditions and we replicate these findings (Soto et al., 2025; Nicks et al., 2024; Krishna et al., 2023). Nicks et al. (2024) in particular highlights a key risk of new detection methods, namely that they become targets to optimize against. Sadasivan et al. (2025) demonstrated that iteratively applying paraphrasing attacks significantly degrades performance. Recently released datasets have pivoted away from

<sup>1</sup>Crucially, the attacks themselves are held out in our evaluations.

evaluating on strictly machine-generated text, and consider cases where humans and LMs may edit and manipulate each others writing (He et al., 2024; Artemova et al., 2025; Dugan et al., 2024; Wu et al., 2024). Prior work has demonstrated that Gaussian Processes trained on feature extractors are effective classifiers for synthetic speech detection (Glazer et al., 2025). Most closely related to our work, Ghostbuster combines several LM derived features for detection, applies a search procedure, and applies a logistic regression to arrive at a final answer (Verma et al., 2024). Our approach differs in that combine distinct feature spaces, and use Gaussian processes which yield calibrated uncertainties with orders of magnitude less data.

### 2.2 Problem Statement

Let  $\mathcal{X}$  denote the space of natural-language documents. We define our *detector* as a function  $h : \mathcal{X} \rightarrow \{0, 1\}$  that maps a document to a binary label, where  $y = 0$  indicates human-written text and  $y = 1$  indicates machine-generated or machine-manipulated text.

**Zero-shot detection.** Most existing detectors operate in a *zero-shot* setting: the detector is applied directly to a test document with no domain-specific training data. Zero-shot methods, such as log-rank tests, likelihood curvature estimates, and cross-perplexity ratios, can easily be run on any generator’s output, in any domain, under any attack, with no adaptation. However, this generality comes at a cost, with performance degrading substantially when the test distribution involves adversarial manipulation.

**Our setting: few-shot, domain-anchored detection.** We adopt a different operating assumption. We assume our system has access to a small *support set* of in-domain documents:

$$\mathcal{S} = \{(x_i, y_i)\}_{i=1}^N, \quad y_i \in \{0, 1\}, \quad (1)$$

$$N = N_H + N_M.$$

where  $N_H$  human-written documents and  $N_M$  machine-generated (and manipulated) documents are drawn from the domain of interest. In our main experiments we use  $N_H = N_M = 32$  documents per class to represent a quantity that is realistic to obtain in most practical scenarios (e.g., a set of known human written essays, verified news articles, or authentic forum posts). We also consider system performance as  $N$  increases to 256 (Figure 2).

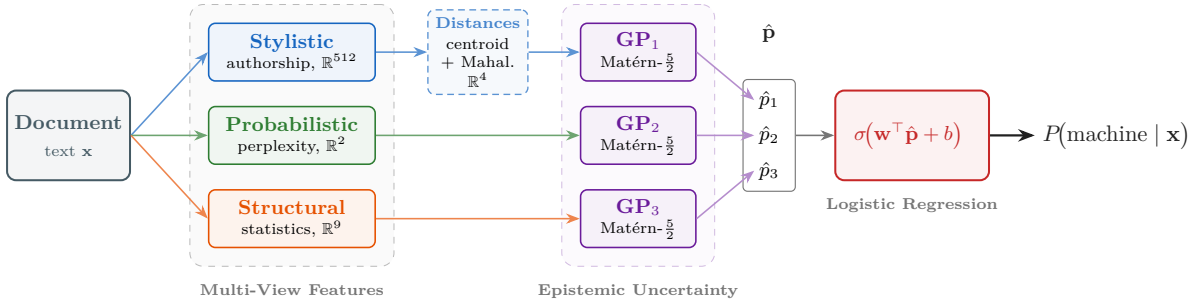


Figure 1: Overview of the proposed approach. Each input  $x$  is represented via three complementary views and transformed into a probability via view-specific GPs. The three scalars are then projected into a single probability via logistic regression.

Crucially, we impose no requirement that the support set reflect the *attack* or the *generator* encountered at test time. This generally aligns with many real-world scenarios, where anticipating all possible generators or attacks isn’t feasible. The human examples must come from the target domain, but the machine examples may be generated by any available model, even one different from the adversary’s generator. In our evaluations, we explicitly hold out both the attack type and the source generator from training, evaluating in a cross-attack and cross-generator transfer setting. That is, we train on a collection of attacks and generators *except* one, and evaluate on that setting. Our key finding is that the GP-based multi-view ensemble is able to leverage this small, potentially mismatched support to generalize robustly to held-out generators and unseen attacks (§4.3).

**Why few-shot?** This formulation takes a middle ground between the zero-shot paradigm (no domain data, broad but fragile coverage) and fully supervised approaches (large labeled corpora, strong but narrow). By anchoring the detector to a small sample from the deployment domain, we provide the model with enough distributional context to learn meaningful decision boundaries, particularly in the centroid based feature space (§3.2), while keeping the data requirement low enough for practical adoption.

### 3 Method

In order to develop a robust detector, we hypothesize that learning to combine the outputs of different models fit on complementary feature spaces will have several advantages over a joint model that learns arbitrary combinations of features across views. First of all, by using independent view-

specific classifiers, an adversary must defeat all views simultaneously to fully evade detection. Second, since we must learn detectors on the basis of small samples of confirmed real and fake data, a model that enabled arbitrary feature combinations would be prone to overfitting those features and therefore generalize poorly.

To this end, we present a multi-view, non-parametric framework for machine-generated text detection. Given a document  $x$ , the system (i) extracts features from  $K$  independent views  $\{\varphi_k\}_{k=1}^K$ , (ii) projects each view into a low-dimensional *distance feature* space, (iii) fits an independent variational Gaussian process (GP) classifier per view, (iv) obtains per-view Bernoulli probabilities  $p_k$  via the probit link, (v) aggregates these probabilities, and (vi) calibrates a decision threshold with finite-sample false-positive guarantees. An out-of-distribution (OOD) gate enables principled abstention when the model encounters text outside its training support.

#### 3.1 Multi-View Feature Extraction

Our approach to selecting views is simple: force an attacker to solve a multi-objective problem due to the different feature spaces of the views. As illustrated in While we use a simple collection of three views, we find that adding additional views helps. Each view  $\varphi_k : \mathcal{X} \rightarrow \mathbb{R}^{D_k}$  maps a raw text document to a feature vector that reflects a distinct axis of variation between human and machine writing. We use  $K = 3$  views:

**Style view** ( $D_k = 4$ ). Dense stylometric embeddings produced by a style representation model<sup>2</sup>, which is trained to encode writing style invariant to topic (Rivera-Soto et al., 2021). These embeddings

<sup>2</sup><https://huggingface.co/rrivera1849/LUAR-CRUD>

capture lexical and syntactic fingerprints that are largely orthogonal to semantic content. To avoid challenges associated with high-dimensional features, we fit centroids based on human and machine data, and compute distances from each centroid for each test point.

**Probabilistic view** ( $D_k = 2$ ). A vector of zero-shot detector scores: (1) the LogRank score, which measures the average token rank under a reference language model, and (2) the FastDetectGPT score, which estimates the log-likelihood curvature around the document. Both scores are computed using Falcon-7B (Almazrouei et al., 2023).

**Structural view** ( $D_k = 8$ ). A vector of hand-crafted document statistics which capture surface-level regularities in document organization that persist through many paraphrase operations, such as total token count and sentence count. Our exact implementation can be found in subsection A.3.

The key motivation for multi-view combination is adversarial robustness. A paraphrase attack that normalizes token-level probability features (the probabilistic view) leaves structural regularities and stylistic fingerprints largely intact. Requiring converging evidence across views therefore raises the cost of any single-axis attack.

### 3.2 Centroid-Based Feature Construction

For high-dimensional embeddings (e.g.,  $D=512$ ), Euclidean distance concentration causes the GP’s kernel to lose discriminative power: pairwise distances converge to a common value, and the GP posterior degenerates toward the prior. A simple solution is to project such views to a low-dimensional space. In more detail, given a labeled support set  $\mathcal{S} = \{(x_i, y_i)\}_{i=1}^N$  (where  $y_i \in \{0, 1\}$  denotes human/machine), for each view  $k$  we first compute class centroids:

$$\begin{aligned}\boldsymbol{\mu}_{H,k} &= \frac{1}{|\mathcal{S}_H|} \sum_{i:y_i=0} \varphi_k(x_i) \\ \boldsymbol{\mu}_{M,k} &= \frac{1}{|\mathcal{S}_M|} \sum_{i:y_i=1} \varphi_k(x_i)\end{aligned}$$

where  $\mathcal{S}_H$  and  $\mathcal{S}_M$  denote the human and machine subsets of the support set, respectively. Each document is mapped to a 4D feature vector combining Euclidean and diagonal Mahalanobis distances to both class centroids:

$$\psi_k(x) = [d_{H,k}, d_{M,k}, m_{H,k}, m_{M,k}] \in \mathbb{R}^4,$$

where  $d_{H,k} = \|\varphi_k(x) - \boldsymbol{\mu}_{H,k}\|_2$  and  $d_{M,k} = \|\varphi_k(x) - \boldsymbol{\mu}_{M,k}\|_2$  are Euclidean distances, and  $m_{H,k} = \|(\varphi_k(x) - \boldsymbol{\mu}_{H,k})/\boldsymbol{\sigma}_{H,k}\|_2$  and  $m_{M,k} = \|(\varphi_k(x) - \boldsymbol{\mu}_{M,k})/\boldsymbol{\sigma}_{M,k}\|_2$  are diagonal Mahalanobis distances, with  $\boldsymbol{\sigma}_{H,k}$  and  $\boldsymbol{\sigma}_{M,k}$  denoting the per-dimension standard deviations of the human and machine support features, respectively. The Mahalanobis components account for per-dimension variance, making the representation sensitive to distributional shape rather than scale alone. Finally, the distance feature vector is standardized (median/MAD); the exact form is given in Appendix A. We denote the standardized features  $\tilde{\psi}_k(x)$ .

### 3.3 Per-View Gaussian Process Classifiers

A separate Gaussian process binary classifier is fit for each view  $k$  on its (optionally distance-reduced) features  $\tilde{\psi}_k$ . We use a sparse variational GP with a Bernoulli likelihood and a probit link (Hensman et al., 2015), a Matérn-5/2 kernel and inducing locations fixed to all  $N$  training points<sup>3</sup>; the variational distribution and kernel parameters are jointly trained by maximizing the evidence lower bound (Titsias, 2009). Full training hyperparameters are listed in Appendix A.

At a test point  $x^*$ , the GP posterior over the latent function gives a predictive mean  $\mu_k(x^*) = \mathbb{E}[f_k(\tilde{\psi}_k(x^*))]$  and variance  $\sigma_k^2(x^*) = \text{Var}[f_k(\tilde{\psi}_k(x^*))]$ . The Bernoulli probability of machine generation for view  $k$  is obtained via the probit link:

$$p_k(x^*) = \Phi\left(\frac{\mu_k(x^*)}{\sqrt{1 + \sigma_k^2(x^*)}}\right),$$

where  $\Phi$  is the standard normal CDF. This probability naturally incorporates the GP’s predictive uncertainty: when  $\sigma_k^2$  is large, the argument to  $\Phi$  is shrunk toward zero, pushing  $p_k$  toward 0.5 and reflecting the model’s lack of confidence. The per-view probabilities  $p_k$  are passed directly to the aggregation stage described next.

### 3.4 Calibration

A simple max or mean over the per-view probabilities  $\{p_k(x^*)\}_{k=1}^K$  ignores systematic differences in calibration across views and is sensitive to a single poorly calibrated GP. We instead learn an

<sup>3</sup>In our regime  $N$  ranges from 8 to 128 per class, so this incurs no scaling concerns.

aggregator in a data-driven manner using a small calibration set.

**Calibration set.** Of the  $2N$  labeled documents available for a (domain, generator) pair we use the first  $N/2$  per class to fit the per-view GPs and hold out the remaining  $N/2$  per class as a calibration set  $\mathcal{C}$ . Because the GPs never see  $\mathcal{C}$ , their predictions on it are unbiased estimates of test-time behavior, eliminating the calibration-leakage failure mode of in-sample stacking.

**Second-stage logistic regression.** For each  $x_i \in \mathcal{C}$  we collect the per-view probability vector  $\mathbf{p}(x_i) = (p_1(x_i), \dots, p_K(x_i)) \in [0, 1]^K$  and fit an  $\ell_2$ -regularized logistic regression. The learned weights expose how much each view contributes to the final detection score and absorb challenges that any individual GP may introduce. This pipeline can be visualized in Figure 1. We also consider alternative aggregation strategies in Appendix C.

### 3.5 Evaluation Protocol

Each trained model is evaluated in a *cross-attack setting*, where the model is evaluated against attacks it has never seen.

**Metrics.** We report partial AUROC at a maximum false-positive rate of 1% (AUROC@1%), which stress-tests the low-FPR regime relevant to high-stakes applications. We observe that AUROC over all operating points becomes saturated, making it difficult to observe changes between detectors. We additionally report Brier score and Expected Calibration Error (ECE) to measure probabilistic calibration (Naeini et al., 2014), lower is better for both of these metrics.

## 4 Experiments

### 4.1 Datasets

We evaluate our approach on a diverse set of datasets, each consisting of several attacks, domains, and language models<sup>4</sup>. **PAN2025** (Bevendorff et al., 2025) The PAN2025 shared task considers five mixtures of human and machine writing: machine-written then human-edited, deeply-mixed text, human-initiated then machine-continued, human-written then machine-polished, and machine-written then machine-

humanized<sup>5</sup>. We focus our evaluations on the held out “human-initiated then machine-continued” (MC) and “human-written then machine-polished” (MP) conditions, using the remaining machine splits to form a machine support.

**RAID** (Dugan et al., 2024) We build custom splits from the publicly released RAID dataset to match our problem statement<sup>6</sup>. Specifically, we sample data from three diverse domains (News, Reddit, and Amazon Reviews) and consider all attacks in the dataset (Dugan et al., 2024). Within each domain, similar to DetectRL, to form a few-shot machine support, we sample exemplars from all attacks except one evaluation attack, the evaluation split contains human data, and machine sample from that attack only. We also control for language model: GPT-4o is held out from all training splits and only included as a held out model during evaluation.

**DetectRL** (Wu et al., 2024) We use the exact splits released by the authors to evaluate our detector<sup>7</sup>. We evaluate on the “Multi-Attack” setting in our main experiments to match the problem statement outlined in subsection 2.2 to control for domain. To form the few-shot machine support, we sample exemplars from all attacks *except* for one evaluation attack, the evaluation split contains human data, and machine samples from that attack only.

### 4.2 Baselines

We compare our approach to several popular zero-shot methods: Binoculars (Hans et al., 2024), Fast-DetectGPT (Bao et al., 2024), Log-Likelihood Log-Rank Ratio (LRR) (Su et al., 2023), Log-Rank (Su et al., 2023), MAGE (Li et al., 2024), RADAR (Hu et al., 2023), ReMoDetect (Lee et al., 2024), and MPU (Tian et al., 2024). Some of these approaches are classifier based, and return interpretable scores between zero and one to discriminate between human and machine text, while others return a raw score. To compute calibration metrics on the latter, we calibrate the raw scores using Platt scaling on held out calibration data (Platt, 1999). Noting that the previous approaches are all zero-shot and do not make use of the data our system uses beyond calibration, we also train a transformer based bi-

<sup>5</sup><https://pan.webis.de/clef25/pan25-web/generated-content-analysis.html>

<sup>6</sup><https://huggingface.co/datasets/liamdugan/raid>

<sup>7</sup><https://github.com/NLP2CT/DetectRL>

<sup>4</sup>We plan to publish our splits alongside our code to reproduce results

Table 1: Detection and calibration performance on the PAN2025 benchmark at  $N=32$  training examples per class.  $\pm$  indicates sample std over three samples. *MC* = machine-continued; *MP* = machine-polished. ECE and Brier are lower-is-better.

Method	<i>MC</i>			<i>MP</i>		
	AUC@1% $\uparrow$	ECE $\downarrow$	Brier $\downarrow$	AUC@1% $\uparrow$	ECE $\downarrow$	Brier $\downarrow$
Binoculars (Hans et al., 2024)	.657 $\pm$ .000	.169 $\pm$ .007	.198 $\pm$ .000	.587 $\pm$ .000	.092 $\pm$ .001	.207 $\pm$ .000
LRR (Su et al., 2023)	.513 $\pm$ .000	.081 $\pm$ .016	.246 $\pm$ .002	.504 $\pm$ .000	.050 $\pm$ .006	.252 $\pm$ .001
Fast-DetectGPT (Bao et al., 2024)	<b>.684</b> $\pm$ .000	.089 $\pm$ .003	.189 $\pm$ .000	.605 $\pm$ .000	.124 $\pm$ .005	.207 $\pm$ .001
Log-Rank (Su et al., 2023)	.500 $\pm$ .000	.092 $\pm$ .024	.247 $\pm$ .001	.503 $\pm$ .000	<b>.034</b> $\pm$ .002	.237 $\pm$ .000
MAGE (Li et al., 2024)	.502 $\pm$ .000	.232 $\pm$ .000	.231 $\pm$ .000	.501 $\pm$ .000	.348 $\pm$ .000	.347 $\pm$ .000
RADAR (Hu et al., 2023)	.547 $\pm$ .000	.183 $\pm$ .000	.232 $\pm$ .000	.502 $\pm$ .000	.317 $\pm$ .000	.352 $\pm$ .000
MPU (Tian et al., 2024)	.530 $\pm$ .000	.436 $\pm$ .000	.432 $\pm$ .000	.591 $\pm$ .000	.363 $\pm$ .000	.360 $\pm$ .000
ReMoDetect (Lee et al., 2024)	.509 $\pm$ .000	.172 $\pm$ .004	.271 $\pm$ .002	.580 $\pm$ .000	.074 $\pm$ .006	.177 $\pm$ .001
RoBERTa-FT	.539 $\pm$ .046	.117 $\pm$ .052	.231 $\pm$ .039	.562 $\pm$ .061	.080 $\pm$ .033	.214 $\pm$ .027
<i>Ours</i>	.612 $\pm$ .009	<b>.080</b> $\pm$ .016	<b>.161</b> $\pm$ .017	<b>.610</b> $\pm$ .028	.096 $\pm$ .011	<b>.177</b> $\pm$ .007

Table 2: Detection and calibration performance on the RAID benchmark at  $N = 32$  training examples per class.  $\pm$  indicates sample std over three samples.

Method	<i>News</i>			<i>Reddit</i>		
	AUC@1% $\uparrow$	ECE $\downarrow$	Brier $\downarrow$	AUC@1% $\uparrow$	ECE $\downarrow$	Brier $\downarrow$
Binoculars (Hans et al., 2024)	.683 $\pm$ .124	.255 $\pm$ .052	.183 $\pm$ .045	.572 $\pm$ .050	.223 $\pm$ .041	.182 $\pm$ .041
LRR (Su et al., 2023)	.513 $\pm$ .020	.137 $\pm$ .089	.243 $\pm$ .045	.510 $\pm$ .008	.152 $\pm$ .052	.198 $\pm$ .040
Fast-DetectGPT (Bao et al., 2024)	.741 $\pm$ .129	<b>.105</b> $\pm$ .100	.113 $\pm$ .110	.649 $\pm$ .115	<b>.095</b> $\pm$ .095	.135 $\pm$ .093
Log-Rank (Su et al., 2023)	.574 $\pm$ .157	.175 $\pm$ .144	.249 $\pm$ .094	.527 $\pm$ .062	.152 $\pm$ .057	.168 $\pm$ .069
MAGE (Li et al., 2024)	.529 $\pm$ .019	.298 $\pm$ .051	.298 $\pm$ .051	.582 $\pm$ .055	.229 $\pm$ .070	.229 $\pm$ .070
RADAR (Hu et al., 2023)	.925 $\pm$ .057	.232 $\pm$ .068	.149 $\pm$ .069	.529 $\pm$ .018	.178 $\pm$ .078	.172 $\pm$ .058
MPU (Tian et al., 2024)	.503 $\pm$ .015	.429 $\pm$ .110	.422 $\pm$ .130	.527 $\pm$ .046	.452 $\pm$ .078	.432 $\pm$ .116
ReMoDetect (Lee et al., 2024)	.577 $\pm$ .069	.213 $\pm$ .056	.273 $\pm$ .010	.687 $\pm$ .128	.259 $\pm$ .105	.167 $\pm$ .102
RoBERTa-FT	.925 $\pm$ .157	.143 $\pm$ .096	.056 $\pm$ .101	.711 $\pm$ .202	.216 $\pm$ .066	.091 $\pm$ .057
<i>Ours</i>	<b>.930</b> $\pm$ .104	.235 $\pm$ .040	<b>.052</b> $\pm$ .028	<b>.775</b> $\pm$ .136	.243 $\pm$ .035	<b>.088</b> $\pm$ .027

nary classifier on the same available to our system by fine-tuning RoBERTa (Liu et al., 2019). Details for this classifier can be found in Appendix B.

### 4.3 Main Experiments

This section describes our experiments across adversarial data splits from the PAN2025 shared task Table 1, RAID benchmark Table 2, and the DetectRL benchmark Table 3. Due to space constraints, we report results for two domains from the RAID dataset in Table 2 and for two attacks from the DetectRL benchmark in Table 3. Additional results with similar trends can be found in Appendix E. Firstly, we confirm findings from previous work and demonstrate that state-of-the-art detectors are brittle to attacks (Krishna et al., 2023; Soto et al., 2025), especially under low FPR operating conditions. The brittleness of these systems extends to calibration, further analysis of this consequence can be found in the following section. Throughout our results, the fine-tuned RoBERTa classifier outperforms most baselines and is most competitive

with our system. We do note that the error bars for this baseline are significantly wider for many conditions, indicating that training is sensitive to the few-shot sample selected. Beyond RoBERTa, across most conditions considered, our few-shot approach significantly outperforms the considered zero-shot baselines under both detection, and calibration metrics.

We report test results on all three datasets, with hyperparameters for our system chosen based on a separate development split of the PAN2025 dataset. Table 1 shows performance under two difficult machine splits: human-initiated and machine-continued (MC) and human-written and machine-polished (MP). These results have the lowest absolute scores relative to other datasets due to the level of mixing human and machine text. Table 2 shows performance for the three considered RAID domains, with performance averaged across all 11 considered attacks. Full results for each attack can be found in Appendix D.

**How does system performance scale with few-**

Table 3: Detection and calibration performance on the DetectRL benchmark at  $N = 32$  training examples per class.  $\pm$  indicates sample std over three samples.

Method	Paraphrase			Perturbation		
	AUC@1% $\uparrow$	ECE $\downarrow$	Brier $\downarrow$	AUC@1% $\uparrow$	ECE $\downarrow$	Brier $\downarrow$
Binoculars (Hans et al., 2024)	.695 $\pm$ .000	.151 $\pm$ .010	.180 $\pm$ .003	.572 $\pm$ .000	.147 $\pm$ .004	.212 $\pm$ .001
LRR (Su et al., 2023)	.616 $\pm$ .000	.135 $\pm$ .006	.229 $\pm$ .001	.510 $\pm$ .000	.038 $\pm$ .014	.250 $\pm$ .001
Fast-DetectGPT (Bao et al., 2024)	.627 $\pm$ .000	.074 $\pm$ .009	.172 $\pm$ .001	.555 $\pm$ .000	.104 $\pm$ .002	.196 $\pm$ .001
Log-Rank (Su et al., 2023)	.587 $\pm$ .000	.095 $\pm$ .046	.244 $\pm$ .001	.500 $\pm$ .000	<b>.036</b> $\pm$ .007	.244 $\pm$ .000
MAGE (Li et al., 2024)	.699 $\pm$ .000	.158 $\pm$ .000	.158 $\pm$ .000	.561 $\pm$ .000	.261 $\pm$ .000	.260 $\pm$ .000
RADAR (Hu et al., 2023)	.706 $\pm$ .000	.141 $\pm$ .000	.135 $\pm$ .000	.634 $\pm$ .000	.194 $\pm$ .000	.178 $\pm$ .000
MPU (Tian et al., 2024)	.632 $\pm$ .000	.262 $\pm$ .000	.273 $\pm$ .000	.521 $\pm$ .000	.402 $\pm$ .000	.409 $\pm$ .000
ReMoDetect (Lee et al., 2024)	.754 $\pm$ .000	<b>.066</b> $\pm$ .001	.141 $\pm$ .000	.634 $\pm$ .000	.039 $\pm$ .006	.139 $\pm$ .001
RoBERTa-FT Classifier	.635 $\pm$ .061	.188 $\pm$ .051	.161 $\pm$ .023	.603 $\pm$ .042	.104 $\pm$ .043	.176 $\pm$ .032
<i>Ours</i>	<b>.804</b> $\pm$ .020	.137 $\pm$ .020	<b>.086</b> $\pm$ .005	<b>.758</b> $\pm$ .038	.124 $\pm$ .014	<b>.114</b> $\pm$ .024

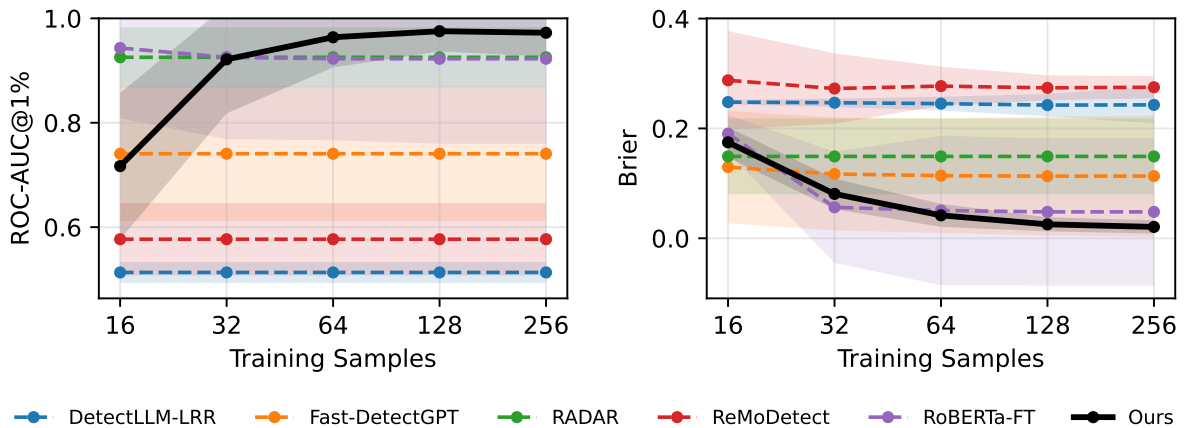


Figure 2: Detection (left) and calibration (right) performance on the News split of the RAID dataset. The GP based approach is able to quickly reach a strong performance point with a small number of training samples, variance of results also decreases significantly with more training samples. Shaded regions show  $\pm 1$  standard error of the mean across different samples and evaluation conditions.

**shot samples?** The baselines we consider are zero-shot, however we do make use of few-shot samples to calibrate these approaches (§4.2). Figure 2 shows system performance against number of few-shot training samples on the News split of the RAID dataset. All approaches are calibrated on the same data, and results are averaged across all 11 attacks. Our approach is able to make use of small amounts of data for detection and there is significantly less variance associated with the selection of this data compared to other methods. Notably, system calibration improves significantly with the number of samples.

**How effectively does our system trade dataset coverage for performance?** We visualize this trade-off using a Performance-Coverage curve, an adaptation of the standard Risk-Coverage formulation (Geifman and El-Yaniv, 2017). Figure 3 shows performance (AUROC@1%) against dataset

coverage on test data consisting of a held out a paraphrasing attack. To generate these curves we rank all test data by each system’s uncertainty, as more of dataset is covered (x-axis), the system is forced to produce responses it is more and more uncertain about. Across the three domains in the RAID dataset we observe that the GP’s uncertainty is indeed informative, as abstention decreases, performance monotonically decreases. We observe that several baselines produce the opposite result with performance increasing as abstention decreases, further confirming poor calibration.

#### How does the system handle far OOD data?

To further understand how well our system handles uncertainty we consider far-OOD data. Our main results feature held out, OOD attacks, but test data is from the same domain as the few-shot exemplars simulating a near-OOD setting. A well calibrated system should be uncertain about pre-

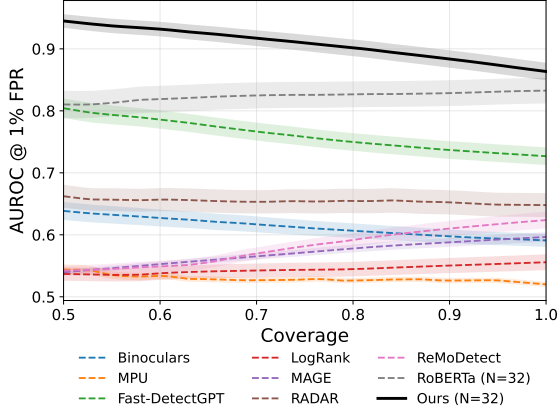


Figure 3: Performance-Coverage curves on the News split of the RAID dataset. Our system demonstrates a monotonically decreasing trend as it is forced to evaluate samples it is increasingly uncertain about.

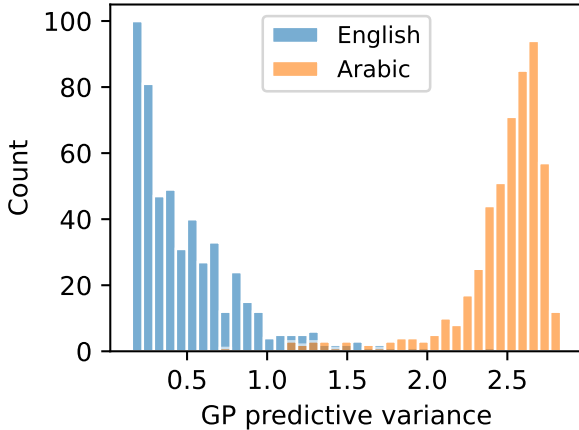


Figure 4: Predictive variance of a GP fit on a style view. English news-wire data is observed during training, at test time far-OOD Arabic data results in significantly higher variances raising the uncertainty of the system.

dictions on far-OOD data, rather than confidently incorrect (e.g., false positives when a detector observes human-written text in a previously unobserved language). To simulate this setting, we introduce human-written and machine-generated Arabic news-wire data from the M4 dataset (Wang et al., 2024). Figure 4 demonstrates how a GP capturing our style view handles the far-OOD data compared to near-OOD data (english data from the News split of the RAID dataset). The posterior variance significantly increases for the Arabic data, which differs stylistically from any of the training data (human or machine).

**How do different views affect system performance?** Table 4 shows an ablation on view configurations. We find that combining views improves

Table 4: Per-view ablation on the RAID dataset. Best per column in **bold**.

Views	AUC	@1%	ECE↓	Brier↓
Probabilistic	0.932	0.773	0.101	0.098
Structural	0.907	0.663	0.203	0.100
Style	0.974	0.685	0.116	0.069
All three	<b>0.996</b>	<b>0.884</b>	<b>0.083</b>	<b>0.030</b>

detection performance across all views.

## 5 Conclusion

Reliable detection of generated texts is complicated by the diversity of text genres, language models, prompting strategies, and evasion techniques. A universal detector covering all conceivable settings may always be vulnerable to a new evasion strategy. This paper addresses a more modest goal: how to developed specialized detectors for specific settings, and how to characterize the data that those detectors will work well on via calibrated uncertainty estimates. To this end, we have shown that the proposed non-parametric approach enables reliable detection using small amounts of human and machine-generated data from the target distribution, that it yields well-calibrated uncertainty estimates, and that the uncertainty estimates can detect both near- and far-OOD data. Our experiments confirm that this is due to two key design choices: (1) the use of multiple complementary views capturing different facets of generated text; (2) the GP classification framework built on top of the distinct feature spaces and then aggregated via a learned calibration map.

## Limitations

We experiment with three views (stylistic, structural, and probabilistic) which our experiments show have complementary benefits enabling robustness to distribution shifts and evasion techniques. Having shown the value of multiple views for robust detection, a natural next step would be experiment with further feature spaces that could provide orthogonal benefits. For example, looking at how features vary within documents could perhaps help detect when editing has taken place. Even with the improved performance of our system, there are significant performance drops in the low FPR operating conditions, which are most like real world scenarios (e.g., plagiarism or cheating accusations in academic settings), more work is needed to validate these systems in such settings. Separately, our

experiments primarily employ existing established benchmarks for machine-text detection, which are primarily English. Our experiments in far-OOD detection suggest that our approach is robust to different languages from those the detector is fit on (appropriately raising uncertainty), but future work should validate the proposed approach in truly multilingual settings.

## References

- Ebtesam Almazrouei, Hamza Alobeidli, Abdulaziz Alshamsi, Alessandro Cappelli, Ruxandra Cojocaru, Mérouane Debbah, Étienne Goffinet, Daniel Hesslow, Julien Launay, Quentin Malartic, Daniele Mazzotta, Badreddine Noune, Baptiste Pannier, and Guilherme Penedo. 2023. [The falcon series of open language models](#). *Preprint*, arXiv:2311.16867.
- Ekaterina Artemova, Jason S Lucas, Saranya Venktraman, Jooyoung Lee, Sergei Tilga, Adaku Uchendu, and Vladislav Mikhailov. 2025. [Beemo: Benchmark of expert-edited machine-generated outputs](#). In *Proceedings of the 2025 Conference of the Nations of the Americas Chapter of the Association for Computational Linguistics: Human Language Technologies (Volume 1: Long Papers)*, pages 6992–7018, Albuquerque, New Mexico. Association for Computational Linguistics.
- Guangsheng Bao, Yanbin Zhao, Zhiyang Teng, Linyi Yang, and Yue Zhang. 2024. [Fast-detectGPT: Efficient zero-shot detection of machine-generated text via conditional probability curvature](#). In *The Twelfth International Conference on Learning Representations*.
- Janek Bevendorff, Daryna Dementieva, Maik Fröbe, Bela Gipp, André Greiner-Petter, Jussi Karlgren, Maximilian Mayerl, Preslav Nakov, Alexander Panchenko, Martin Potthast, Artem Shelmanov, Efstathios Stamatatos, Benno Stein, Yuxia Wang, Matti Wiegmann, and Eva Zangerle. 2025. [Overview of pan 2025: Voight-kampff generative ai detection, multilingual text detoxification, multi-author writing style analysis, and generative plagiarism detection](#). In *Experimental IR Meets Multilinguality, Multimodality, and Interaction: 16th International Conference of the CLEF Association, CLEF 2025, Madrid, Spain, September 9–12, 2025, Proceedings*, page 388–411, Berlin, Heidelberg. Springer-Verlag.
- Gheorghe Comanici and 1 others. 2025. [Gemini 2.5: Pushing the frontier with advanced reasoning, multimodality, long context, and next generation agentic capabilities](#). *Preprint*, arXiv:2507.06261.
- Liam Dugan, Alyssa Hwang, Filip Trhlfk, Andrew Zhu, Josh Magnus Ludan, Hainiu Xu, Daphne Ippolito, and Chris Callison-Burch. 2024. [RAID: A shared benchmark for robust evaluation of machine-generated text detectors](#). In *Proceedings of the 62nd Annual Meeting of the Association for Computational Linguistics (Volume 1: Long Papers)*, pages 12463–12492, Bangkok, Thailand. Association for Computational Linguistics.
- Bradley Emi and Max Spero. 2024. [Technical report on the pangram ai-generated text classifier](#). *Preprint*, arXiv:2402.14873.
- Lukas Gehring and Benjamin Paaßen. 2025. [Assessing llm text detection in educational contexts: Does human contribution affect detection?](#) *Preprint*, arXiv:2508.08096.
- Sebastian Gehrmann, Hendrik Strobelt, and Alexander Rush. 2019. [GLTR: Statistical detection and visualization of generated text](#). In *Proceedings of the 57th Annual Meeting of the Association for Computational Linguistics: System Demonstrations*, pages 111–116, Florence, Italy. Association for Computational Linguistics.
- Yonatan Geifman and Ran El-Yaniv. 2017. Selective classification for deep neural networks. In *Proceedings of the 31st International Conference on Neural Information Processing Systems, NIPS’17*, page 4885–4894, Red Hook, NY, USA. Curran Associates Inc.
- Neta Glazer, David Chernin, Idan Achituve, Sharon Gannot, and Ethan Fetaya. 2025. [Few-shot speech deepfake detection adaptation with gaussian processes](#). *Preprint*, arXiv:2505.23619.
- Aaron Grattafiori and 1 others. 2024. [The llama 3 herd of models](#). *Preprint*, arXiv:2407.21783.
- Abhimanyu Hans, Avi Schwarzschild, Valeriia Cherepanova, Hamid Kazemi, Aniruddha Saha, Micah Goldblum, Jonas Geiping, and Tom Goldstein. 2024. [Spotting llms with binoculars: Zero-shot detection of machine-generated text](#). *Preprint*, arXiv:2401.12070.
- Xinlei He, Xinyue Shen, Zeyuan Chen, Michael Backes, and Yang Zhang. 2024. [Mgtbench: Benchmarking machine-generated text detection](#). *Preprint*, arXiv:2303.14822.
- James Hensman, Alexander Matthews, and Zoubin Ghahramani. 2015. [Scalable Variational Gaussian Process Classification](#). In *Proceedings of the Eighteenth International Conference on Artificial Intelligence and Statistics*, volume 38 of *Proceedings of Machine Learning Research*, pages 351–360, San Diego, California, USA. PMLR.
- Xiaomeng Hu, Pin-Yu Chen, and Tsung-Yi Ho. 2023. [RADAR: Robust AI-text detection via adversarial learning](#). In *Thirty-seventh Conference on Neural Information Processing Systems*.
- Daphne Ippolito, Daniel Duckworth, Chris Callison-Burch, and Douglas Eck. 2020. [Automatic detection of generated text is easiest when humans are fooled](#). In *Proceedings of the 58th Annual Meeting of*

- the Association for Computational Linguistics*, pages 1808–1822, Online. Association for Computational Linguistics.
- John Kirchenbauer, Jonas Geiping, Yuxin Wen, Jonathan Katz, Ian Miers, and Tom Goldstein. 2023. [A watermark for large language models](#). In *Proceedings of the 40th International Conference on Machine Learning*, volume 202 of *Proceedings of Machine Learning Research*, pages 17061–17084. PMLR.
- Kalpesh Krishna, Yixiao Song, Marzena Karpinska, John Frederick Wieting, and Mohit Iyyer. 2023. [Paraphrasing evades detectors of AI-generated text, but retrieval is an effective defense](#). In *Thirty-seventh Conference on Neural Information Processing Systems*.
- Hyunseok Lee, Jihoon Tack, and Jinwoo Shin. 2024. [Remodetect: Reward models recognize aligned LLM’s generations](#). In *The Thirty-eighth Annual Conference on Neural Information Processing Systems*.
- Yafu Li, Qintong Li, Leyang Cui, Wei Bi, Zhilin Wang, Longyue Wang, Linyi Yang, Shuming Shi, and Yue Zhang. 2024. [MAGE: Machine-generated text detection in the wild](#). In *Proceedings of the 62nd Annual Meeting of the Association for Computational Linguistics (Volume 1: Long Papers)*, pages 36–53, Bangkok, Thailand. Association for Computational Linguistics.
- Yinhan Liu, Myle Ott, Naman Goyal, Jingfei Du, Mandar Joshi, Danqi Chen, Omer Levy, Mike Lewis, Luke Zettlemoyer, and Veselin Stoyanov. 2019. [Roberta: A robustly optimized bert pretraining approach](#). *Preprint*, arXiv:1907.11692.
- Eric Mitchell, Yoonho Lee, Alexander Khazatsky, Christopher D. Manning, and Chelsea Finn. 2023. [Detectgpt: Zero-shot machine-generated text detection using probability curvature](#). *Preprint*, arXiv:2301.11305.
- Mahdi Pakdaman Naeini, Gregory F. Cooper, and Milos Hauskrecht. 2014. [Binary classifier calibration: Non-parametric approach](#). *Preprint*, arXiv:1401.3390.
- Charlotte Nicks, Eric Mitchell, Rafael Rafailov, Archit Sharma, Christopher D Manning, Chelsea Finn, and Stefano Ermon. 2024. [Language model detectors are easily optimized against](#). In *The Twelfth International Conference on Learning Representations*.
- OpenAI and 1 others. 2024. [Gpt-4 technical report](#). *Preprint*, arXiv:2303.08774.
- Ajay Patel, Nicholas Andrews, and Chris Callison-Burch. 2024. [Low-resource authorship style transfer: Can non-famous authors be imitated?](#) *Preprint*, arXiv:2212.08986.
- John Platt. 1999. [Probabilistic outputs for support vector machines and comparisons to regularized likelihood methods](#).
- Rafael A. Rivera-Soto, Olivia Elizabeth Miano, Juanita Ordonez, Barry Y. Chen, Aleem Khan, Marcus Bishop, and Nicholas Andrews. 2021. [Learning universal authorship representations](#). In *Proceedings of the 2021 Conference on Empirical Methods in Natural Language Processing*, pages 913–919, Online and Punta Cana, Dominican Republic. Association for Computational Linguistics.
- Vinu Sankar Sadasivan, Aounon Kumar, Sriram Balasubramanian, Wenxiao Wang, and Soheil Feizi. 2025. [Can AI-generated text be reliably detected? stress testing AI text detectors under various attacks](#). *Transactions on Machine Learning Research*.
- Irene Solaiman, Miles Brundage, Jack Clark, Amanda Askell, Ariel Herbert-Voss, Jeff Wu, Alec Radford, Gretchen Krueger, Jong Wook Kim, Sarah Kreps, and 1 others. 2019. [Release strategies and the social impacts of language models](#). *arXiv preprint arXiv:1908.09203*.
- Rafael Alberto Rivera Soto, Kailin Koch, Aleem Khan, Barry Y. Chen, Marcus Bishop, and Nicholas Andrews. 2024. [Few-shot detection of machine-generated text using style representations](#). In *The Twelfth International Conference on Learning Representations*.
- Rafael Rivera Soto, Barry Chen, and Nicholas Andrews. 2025. [Language models optimized to fool detectors still have a distinct style \(and how to change it\)](#). *Preprint*, arXiv:2505.14608.
- Jinyan Su, Terry Yue Zhuo, Di Wang, and Preslav Nakov. 2023. [DetectLLM: Leveraging log rank information for zero-shot detection of machine-generated text](#). In *The 2023 Conference on Empirical Methods in Natural Language Processing*.
- Katherine Thai, Bradley Emi, Elyas Masrouf, and Mohit Iyyer. 2026. [Editlens: Quantifying the extent of AI editing in text](#). In *The Fourteenth International Conference on Learning Representations*.
- Yuchuan Tian, Hanting Chen, Xutao Wang, Zheyuan Bai, QINGHUA ZHANG, Ruifeng Li, Chao Xu, and Yunhe Wang. 2024. [Multiscale positive-unlabeled detection of AI-generated texts](#). In *The Twelfth International Conference on Learning Representations*.
- Michalis Titsias. 2009. [Variational learning of inducing variables in sparse gaussian processes](#). In *Proceedings of the Twelfth International Conference on Artificial Intelligence and Statistics*, volume 5 of *Proceedings of Machine Learning Research*, pages 567–574, Hilton Clearwater Beach Resort, Clearwater Beach, Florida USA. PMLR.
- Vivek Verma, Eve Fleisig, Nicholas Tomlin, and Dan Klein. 2024. [Ghostbuster: Detecting text ghostwritten by large language models](#). In *Proceedings of the 2024 Conference of the North American Chapter of the Association for Computational Linguistics: Human Language Technologies (Volume 1: Long Papers)*, pages 1702–1717, Mexico City, Mexico. Association for Computational Linguistics.

Tianchun Wang, Yuanzhou Chen, Zichuan Liu, Zhanwen Chen, Haifeng Chen, Xiang Zhang, and Wei Cheng. 2025. [Humanizing the machine: Proxy attacks to mislead LLM detectors](#). In *The Thirteenth International Conference on Learning Representations*.

Yuxia Wang, Jonibek Mansurov, Petar Ivanov, Jinyan Su, Artem Shelmanov, Akim Tsvigun, Chenxi Whitehouse, Osama Mohammed Afzal, Tarek Mahmoud, Toru Sasaki, Thomas Arnold, Alham Fikri Aji, Nizar Habash, Iryna Gurevych, and Preslav Nakov. 2024. [M4: Multi-generator, multi-domain, and multilingual black-box machine-generated text detection](#). In *Proceedings of the 18th Conference of the European Chapter of the Association for Computational Linguistics (Volume 1: Long Papers)*, pages 1369–1407, St. Julian’s, Malta. Association for Computational Linguistics.

Junchao Wu, Runzhe Zhan, Derek F. Wong, Shu Yang, Xinyi Yang, Yulin Yuan, and Lidia S. Chao. 2024. [DetectRL: Benchmarking LLM-generated text detection in real-world scenarios](#). In *The Thirty-eight Conference on Neural Information Processing Systems Datasets and Benchmarks Track*.

Xianjun Yang, Wei Cheng, Yue Wu, Linda Ruth Petzold, William Yang Wang, and Haifeng Chen. 2024. [DNA-GPT: Divergent n-gram analysis for training-free detection of GPT-generated text](#). In *The Twelfth International Conference on Learning Representations*.

## A Gaussian Process Training Details

### A.1 Robust Standardization of Distance Features

Before being passed to the per-view GP kernels, the distance features  $\psi_k(x)$  defined in Section 3.2 are normalized to a dimensionless scale using the support set’s median and median absolute deviation (MAD):

$$\tilde{\psi}_k(x) = \frac{\psi_k(x) - \text{median}[\psi_k(\mathcal{S})]}{\text{MAD}[\psi_k(\mathcal{S})] \times 1.4826}, \quad (2)$$

where the factor 1.4826 makes the MAD consistent with the standard deviation under Gaussian data. The use of median/MAD rather than mean/standard deviation makes the standardization robust to the heavy-tailed distance distributions that arise under adversarial attacks. This maps all views to a common scale, making GP kernel hyperparameters and predictive probabilities directly comparable across views.

### A.2 Training Hyperparameters

Table 5 lists the hyperparameters used to train each per-view GP. The same settings are used for every

Hyperparameter	Value
Kernel	Matérn-5/2
Likelihood	Bernoulli (probit link)
Training Samples	$\leq 256$
Variational distribution	Cholesky
Optimizer	Adam
Learning rate	0.01
Max epochs	500
Early stopping patience	20 epochs
Early stopping min. delta	$10^{-4}$

Table 5: Per-view GP training hyperparameters.

Feature	Definition
Doc length	Number of word tokens.
Sentence count	Number of sentences.
Paragraph count	Number of paragraphs.
Mean sentence length	Mean words per sentence.
Std. sentence length	Population std. of sent.
Punctuation density	Count of { , , ; , - , - }.
Type-token ratio	$ \text{unique tokens} / \text{tokens} $ .
Mean word length	Mean chars per word.

Table 6: Per-document structural features. Each document is represented as an  $\mathbb{R}^8$  vector.

view, dataset, and training-set size in our experiments. All experiments were conducted on a single V100 GPU.

### A.3 Structural View Implementation

The structural view summarizes each document with eight surface-level features that are cheap to compute and require no learned model. Tokenization uses NLTK’s `punkt_tab` sentence and word tokenizers; paragraphs are approximated by splitting on double newlines. Table 6 lists the features.

## B Baseline Classifier Training Details

We fine-tune RoBERTa-base on the exact same data splits seen by our system<sup>8</sup>. We train for 10 epochs using the AdamW optimizer and a learning rate of  $2e^{-5}$ .

## C Alternative Aggregation Strategies

Here we explore several alternative approaches to aggregating features and probabilities across views. Table 7 shows cross-attack performance with these strategies. First we consider eliminating the multi-classifier approach in favor of concatenated features fed to either a logistic regression or multi-layer perceptron (MLP) "LR/MLP (Concat)". This gives the system the ability to see all features at

<sup>8</sup><https://huggingface.co/FacebookAI/roberta-base>

the same time, but makes single-view attacks more difficult to identify as out of distribution. We then consider replacing the multi-GP configuration with a multiple logistic regression or multiple MLP classifier with mean pooled probabilities. We find that the stacked GP configuration provides the most consistent performance.

## D Additional RAID Experiments

Table 2 averages results over the 11 considered attacks in the RAID benchmark. We breakdown performance across those attacks in Table 8, Table 9, and Table 10.

## E Additional Domains and Attacks

Due to space limitations, Table 2 only reported results on two domains and Table 3 only reported results on two attacks. We report an additional domain from the RAID dataset (Table 11) and attack from the DetectRL benchmark (Table 12). The results on these extra splits share similar trends with our main experiments in subsection 4.3.

Table 7: DetectRL Cross-Attack Generalization with various aggregation strategies. **Bold** indicates best performance, underline indicates 2nd best per column. *Data Mix* attack does not contain in-domain data.

Eval	Method	AUCROC	AUROC@1	ECE	Brier
<i>Paraphrase</i>	LR (Concat)	0.9676	0.8327	<b>0.0388</b>	<u>0.0675</u>
	LR (Per-View)	0.9726	0.8326	0.1767	0.1003
	MLP (Concat)	0.9669	0.8027	0.0539	0.0731
	MLP (Per-View)	<u>0.9751</u>	<u>0.8451</u>	0.1527	0.0881
	GP (Concat)	0.9689	0.7665	0.0817	0.0765
	GP (Per-View)	<u>0.9762</u>	0.8343	0.2233	0.1129
	GP (Stacking)	<b>0.9847</b>	<b>0.8656</b>	<u>0.0529</u>	<b>0.0493</b>
<i>Perturbation</i>	LR (Concat)	0.9703	0.8273	0.0723	0.0782
	LR (Per-View)	0.9638	0.8067	0.1755	0.1158
	MLP (Concat)	0.9629	0.7589	<b>0.0686</b>	0.0876
	MLP (Per-View)	<u>0.9741</u>	<u>0.8397</u>	0.1647	0.1003
	GP (Concat)	0.9723	0.8186	0.0777	<u>0.0753</u>
	GP (Per-View)	<u>0.9763</u>	<u>0.8493</u>	0.2157	0.1149
	GP (Stacking)	<b>0.9770</b>	<b>0.8618</b>	<u>0.0693</u>	<b>0.0673</b>
<i>Prompt</i>	LR (Concat)	0.9401	<u>0.8424</u>	<u>0.0630</u>	0.0921
	LR (Per-View)	0.9453	0.8081	0.1398	0.1140
	MLP (Concat)	<u>0.9510</u>	<b>0.8434</b>	0.0721	0.0894
	MLP (Per-View)	<u>0.9475</u>	0.7951	0.1096	<u>0.1026</u>
	GP (Concat)	<u>0.9521</u>	0.7344	0.0768	0.0909
	GP (Per-View)	0.9429	0.7731	0.1768	0.1271
	GP (Stacking)	<b>0.9552</b>	0.8042	<b>0.0444</b>	<b>0.0792</b>
<i>Data Mix</i>	LR (Concat)	0.9372	<b>0.7710</b>	<u>0.0438</u>	0.0976
	LR (Per-View)	0.9376	<u>0.7469</u>	0.1485	0.1248
	MLP (Concat)	0.9415	<u>0.7322</u>	0.0839	0.1025
	MLP (Per-View)	<u>0.9474</u>	0.7212	0.1447	0.1112
	GP (Concat)	0.9390	0.7017	0.0439	<u>0.0969</u>
	GP (Per-View)	<u>0.9483</u>	0.7192	0.1930	<u>0.1300</u>
	GP (Stacking)	<b>0.9532</b>	0.7331	<b>0.0379</b>	<b>0.0829</b>

Table 8: AUROC@1% per attack — *News* split of RAID dataset. Italics indicate near-chance performance ( $< 0.55$ ).

	AltSpell	ArtDel	Homoglyph	InsPara	Number	Paraphrase	PplxMisp	Synonym	UpLower	Whitespace	ZeroWidth
MPU (Tian et al., 2024)	0.500	0.499	0.497	0.498	0.500	0.551	0.498	0.497	0.497	0.497	0.497
Binoculars (Hans et al., 2024)	0.746	0.611	0.507	0.714	0.744	0.839	0.723	0.499	0.636	0.591	0.904
LRR (Su et al., 2023)	0.507	0.499	0.536	0.506	0.507	0.516	0.503	0.498	0.498	0.508	0.567
Fast-DetectGPT (Bao et al., 2024)	0.792	0.649	0.653	0.763	0.791	<b>0.886</b>	0.768	0.500	0.688	0.663	0.999
Log-Rank (Su et al., 2023)	0.513	0.499	0.765	0.514	0.510	0.512	0.506	0.497	0.498	0.498	<b>1.000</b>
MAGE (Li et al., 2024)	0.535	0.511	0.497	0.536	0.538	0.566	0.526	0.513	0.509	0.536	0.546
RADAR (Hu et al., 2023)	0.952	0.921	0.876	0.964	0.957	0.777	0.947	0.920	0.959	0.907	0.999
ReMoDetect (Lee et al., 2024)	0.645	0.554	0.497	0.665	0.626	0.533	0.643	0.497	0.523	0.665	0.497
Ours	<b>0.997</b>	<b>0.981</b>	<b>0.999</b>	<b>0.988</b>	<b>0.991</b>	0.880	<b>0.985</b>	<b>0.943</b>	<b>0.982</b>	<b>0.984</b>	<b>1.000</b>

Table 9: AUROC@1% per attack — *Reddit* split of RAID dataset. Italics indicate near-chance performance (< 0.55).

	AltSpell	ArtDel	Homoglyph	InsPara	Number	Paraphrase	PplxMisp	Synonym	UpLower	Whitespace	ZeroWidth
MPU (Tian et al., 2024)	<i>0.504</i>	<i>0.503</i>	0.598	<i>0.503</i>	<i>0.506</i>	<i>0.544</i>	<i>0.502</i>	<i>0.502</i>	<i>0.500</i>	<i>0.498</i>	0.637
Binoculars (Hans et al., 2024)	0.615	0.568	<i>0.498</i>	0.599	0.632	0.609	0.595	<i>0.500</i>	<i>0.538</i>	<i>0.514</i>	0.628
LRR (Su et al., 2023)	<i>0.510</i>	<i>0.505</i>	<i>0.510</i>	<i>0.511</i>	<i>0.512</i>	<i>0.520</i>	<i>0.508</i>	<i>0.499</i>	<i>0.502</i>	<i>0.509</i>	<i>0.531</i>
Fast-DetectGPT (Bao et al., 2024)	0.676	0.607	0.555	0.658	0.699	0.702	0.651	<i>0.500</i>	0.580	0.563	<b>0.949</b>
Log-Rank (Su et al., 2023)	<i>0.504</i>	<i>0.502</i>	0.570	<i>0.504</i>	<i>0.504</i>	<i>0.504</i>	<i>0.503</i>	<i>0.498</i>	<i>0.499</i>	<i>0.500</i>	0.709
MAGE (Li et al., 2024)	0.594	<i>0.549</i>	<i>0.497</i>	0.615	0.614	0.687	0.554	<i>0.535</i>	<i>0.516</i>	0.615	0.630
RADAR (Hu et al., 2023)	0.550	<i>0.541</i>	<i>0.499</i>	<i>0.548</i>	0.553	<i>0.530</i>	<i>0.536</i>	<i>0.527</i>	<i>0.523</i>	<i>0.515</i>	<i>0.498</i>
ReMoDetect (Lee et al., 2024)	0.798	0.745	<i>0.497</i>	0.814	0.809	0.651	0.772	<i>0.515</i>	0.645	0.814	<i>0.497</i>
Ours	<b>0.901</b>	<b>0.821</b>	<b>0.859</b>	<b>0.897</b>	<b>0.961</b>	<b>0.736</b>	<b>0.894</b>	<b>0.560</b>	<b>0.848</b>	<b>0.816</b>	0.633

Table 10: AUROC@1% per attack — *Reviews* split of RAID dataset. Italics indicate near-chance performance (< 0.55).

	AltSpell	ArtDel	Homoglyph	InsPara	Number	Paraphrase	PplxMisp	Synonym	UpLower	Whitespace	ZeroWidth
MPU(Tian et al., 2024)	<i>0.506</i>	<i>0.500</i>	0.583	<i>0.499</i>	<i>0.514</i>	0.638	<i>0.508</i>	<i>0.506</i>	<i>0.498</i>	<i>0.497</i>	0.575
Binoculars(Hans et al., 2024)	<i>0.533</i>	<i>0.504</i>	<i>0.497</i>	<i>0.531</i>	0.567	<i>0.512</i>	<i>0.541</i>	<i>0.497</i>	<i>0.504</i>	<i>0.499</i>	0.528
LRR(Su et al., 2023)	<i>0.497</i>	<i>0.497</i>	<i>0.513</i>	<i>0.497</i>	<i>0.497</i>	<i>0.498</i>	<i>0.497</i>	<i>0.497</i>	<i>0.497</i>	<i>0.498</i>	0.595
Fast-DetectGPT(Bao et al., 2024)	0.844	0.728	0.554	0.871	0.921	<b>0.897</b>	0.879	<i>0.505</i>	0.771	0.729	<b>1.000</b>
Log-Rank(Su et al., 2023)	<i>0.504</i>	<i>0.498</i>	<b>0.783</b>	<i>0.505</i>	<i>0.508</i>	<i>0.506</i>	<i>0.503</i>	<i>0.497</i>	<i>0.497</i>	<i>0.499</i>	0.928
MAGE(Li et al., 2024)	0.629	<i>0.516</i>	<i>0.497</i>	0.646	0.645	0.705	0.626	0.594	<i>0.524</i>	0.646	0.670
RADAR(Hu et al., 2023)	<i>0.497</i>	<i>0.497</i>	<i>0.497</i>	<i>0.497</i>	<i>0.497</i>	<i>0.497</i>	<i>0.497</i>	<i>0.497</i>	<i>0.497</i>	<i>0.497</i>	<i>0.497</i>
ReMoDetect(Lee et al., 2024)	0.786	0.712	<i>0.497</i>	0.807	0.804	0.609	0.793	<i>0.546</i>	0.694	0.807	<i>0.497</i>
Ours	<b>0.982</b>	<b>0.905</b>	0.714	<b>0.984</b>	<b>0.990</b>	0.788	<b>0.989</b>	<b>0.601</b>	<b>0.981</b>	<b>0.951</b>	0.984

Table 11: Detection and calibration performance on the RAID *Reviews* domain at  $N = 32$  training examples per class.  $\pm$  indicates sample std over three samples.

Method	AUC@1% $\uparrow$	ECE $\downarrow$	Brier $\downarrow$
Binoculars (Hans et al., 2024)	.518 $\pm$ .020	.264 $\pm$ .046	.176 $\pm$ .044
LRR (Su et al., 2023)	.508 $\pm$ .027	.235 $\pm$ .075	.263 $\pm$ .074
Fast-DetectGPT (Bao et al., 2024)	.791 $\pm$ .148	<b>.103</b> $\pm$ .090	.098 $\pm$ .099
Log-Rank (Su et al., 2023)	.566 $\pm$ .142	.198 $\pm$ .106	.226 $\pm$ .102
MAGE (Li et al., 2024)	.609 $\pm$ .066	.161 $\pm$ .070	.159 $\pm$ .070
RADAR (Hu et al., 2023)	.497 $\pm$ .000	.208 $\pm$ .100	.171 $\pm$ .084
MPU (Tian et al., 2024)	.530 $\pm$ .046	.415 $\pm$ .104	.388 $\pm$ .136
ReMoDetect (Lee et al., 2024)	.687 $\pm$ .123	.326 $\pm$ .120	.174 $\pm$ .133
RoBERTa-FT	.861 $\pm$ .205	.215 $\pm$ .070	.087 $\pm$ .053
<i>Ours</i>	<b>.895</b> $\pm$ .140	.232 $\pm$ .037	<b>.079</b> $\pm$ .033

Table 12: Detection and calibration performance on the DetectRL *Prompt* attack at  $N = 32$  training examples per class.  $\pm$  indicates sample std over three samples.

Method	AUC@1% $\uparrow$	ECE $\downarrow$	Brier $\downarrow$
Binoculars (Hans et al., 2024)	.805 $\pm$ .000	.140 $\pm$ .001	.132 $\pm$ .000
LRR (Su et al., 2023)	.688 $\pm$ .000	.091 $\pm$ .007	.178 $\pm$ .002
Fast-DetectGPT (Bao et al., 2024)	.746 $\pm$ .000	<b>.046</b> $\pm$ .001	.124 $\pm$ .000
Log-Rank (Su et al., 2023)	.684 $\pm$ .000	.060 $\pm$ .001	.153 $\pm$ .000
MAGE (Li et al., 2024)	.758 $\pm$ .000	.159 $\pm$ .000	.159 $\pm$ .000
RADAR (Hu et al., 2023)	.671 $\pm$ .000	.191 $\pm$ .000	.188 $\pm$ .000
MPU (Tian et al., 2024)	.637 $\pm$ .000	.243 $\pm$ .000	.248 $\pm$ .000
ReMoDetect (Lee et al., 2024)	.801 $\pm$ .000	.050 $\pm$ .005	.104 $\pm$ .000
RoBERTa-FT Classifier	.733 $\pm$ .115	.206 $\pm$ .069	.188 $\pm$ .023
<i>Ours</i>	<b>.809</b> $\pm$ .025	.120 $\pm$ .031	<b>.100</b> $\pm$ .010